Synthesis and Structural Characterization of a Novel Dodecaosmium Carbonyl Cluster $[Os_{12}(CO)_{30}]$ Derived from a New μ_4-Oxo Hexaosmium Carbonyl Cluster $[Os_6(CO)_{16}(\mu_4\text{-}O)(\mu\text{-}OH)_2(\mu\text{-}CO)_2]$

Janet Shuk-Yee Wong,[†] Zhen-Yang Lin,[‡] and Wing-Tak Wong*[,†]

Department of Chemistry, The University of Hong Kong, Pokfulam Road, Hong Kong, People's Republic of China, and Department of Chemistry, The University of Science and Technology, Clear Water Bay, Hong Kong, People's Republic of China

Received April 15, 2003

A novel hexaosmium μ_4-oxo cluster, $[Os_6(CO)_{16}(\mu_4\text{-}O)(\mu\text{-}OH)_2(\mu\text{-}CO)_2]$, **1**, was isolated from the reaction of $[Os_3(CO)_{11}(NCMe)]$ and O_2 in refluxing octane. Vacuum pyrolysis of **1** afforded a new highest nuclearity neutral binary osmium cluster, $[Os_{12}(CO)_{30}]$, **2**, in moderate yield. Both clusters were fully characterized by both spectroscopic and crystallographic techniques. Molecular orbital calculations were performed on **1**, which was two electrons in excess according to the effective atomic number rule. The redox properties of **1** were investigated by means of cyclic voltammetry and controlled potential coulometry.

Introduction

Metal clusters that contain oxo ligands are of considerable interest because they can serve as models for intermediates in catalytic oxidation or as reagents and catalysts in the oxidation of organic compounds.[1−4] However, in osmium systems, the chemistry of high-nuclearity oxo clusters has not been well investigated. Even though the metal has been known to undergo oxidation under ambient conditions, the reactivity of metal cluster species with molecular oxygen is largely unexplored.[1b,e,5,6] In recent decades, binary high-nuclearity osmium carbonyl clusters have been effectively synthesized by the pyrolysis of $[Os_3(CO)_{12}]$ and its derivatives.[7] Clusters of up to 20 osmium atoms have been prepared by this method. However, higher nuclearity clusters (>9) tend to form anions. Neutral carbonyl clusters are thought to be rather difficult to isolate and to fully characterize due to limited solubility and stability. We recently developed a synthetic route to a new hexaosmium oxo cluster in moderate yield, and its pyrolysis reaction has been studied. In this communication, we present the syntheses and structural characterization of the novel hexanuclear oxo cluster $[Os_6(CO)_{16}(\mu_4\text{-}O)(\mu\text{-}OH)_2(\mu\text{-}CO)_2]$, **1**, and the neutral high-nuclearity osmium cluster $[Os_{12}(CO)_{30}]$, **2**.

Results and Discussion

Synthesis of $[Os_6(CO)_{16}(\mu_4\text{-}O)(\mu\text{-}OH)_2(\mu\text{-}CO)_2]$, 1. The triosmium cluster $[Os_3(CO)_{11}(NCMe)]$ was allowed to react with a continuous stream of oxygen in octane under reflux for 15 min, and the new μ_4-oxo hexaosmium cluster $[Os_6(CO)_{16}(\mu_4\text{-}O)(\mu\text{-}OH)_2(\mu\text{-}CO)_2]$, **1**, was isolated in 55% yield. Purple crystals of **1** that were suitable for a single-crystal X-ray analysis were obtained by recrystallization from CH_2Cl_2−hexane at 0 °C.

The molecular structure of **1** is shown in Figure 1, and some important bond parameters are given in Table 1. One molecule of CH_2Cl_2, as a solvent of crystallization, was found in the crystal lattice. The metal framework of **1** consists of an $Os_4(CO)_8(\mu_4\text{-}O)$ unit, and the tetraosmium plane, Os(3)−Os(4)−Os(5)−Os(6), is slightly twisted with a maximum deviation from the least-squares plane of 0.034 Å. The bond lengths of the opposite edges Os(3)−Os(6) and Os(4)−Os(5) are almost the same [2.981(1) vs 2.986(1) Å], and both are

* Corresponding author. E-mail: wtwong@hkucc.hku.hk. Fax: (852) 2547 2933.
[†] The University of Hong Kong.
[‡] The University of Science and Technology.

(1) (a) Mirza, H. A.; Vittal, J. J.; Puddephatt, R. J. *Inorg. Chem.* **1995**, *34*, 4239−4243. (b) Ingham, S. L.; Lewis, J.; Raithby, P. R. *J. Chem. Soc., Chem. Commun.* **1993**, 166−167. (c) Park, J. T.; Chi, Y.; Shapley, J. R.; Churchill, M. R.; Ziller, J. W. *Organometallics* **1994**, *13*, 813−821. (d) Belli Dell'Amico, D.; Bradicich, C.; Calderazzo, F.; Guarini, A.; Labella, L.; Marchetti, F.; Tomei, A. *Inorg. Chem.* **2002**, *41*, 2814−2816. (e) Goudsmit, R. J.; Johnson, B. F. G.; Lewis, J.; Raithby, P. R.; Whitmire, K. H. *J. Chem. Soc., Chem. Commun.* **1983**, 246−247. (f) Faure, M.; Jahncke, M.; Neels, A.; Stoeckli-Evans, H.; Süss-Fink, G. *Polyhedron* **1999**, *18*, 2679−2685. (g) Schauer, C. K.; Voss, E. J.; Sabat, M.; Shriver, D. F. *Inorg. Chim. Acta* **2000**, *300*−*302*, 7−15. (h) Adams, H.; Gill, L. J.; Morris, M. J. *J. Organomet. Chem.* **1997**, *533*, 117−123.

(2) (a) Budzichowski, T. A.; Chisholm, M. H.; Streib, W. E. *J. Am. Chem. Soc.* **1994**, *116*, 389−390. (b) Li, J. J.; Sharp, P. R. *Inorg. Chem.* **1994**, *33*, 183−184.

(3) Bottomley, F.; Boyle, P. D.; Chen, J. H. *Organometallics* **1994**, *13*, 370−373.

(4) (a) Griffith, W. P. *Chem. Soc. Rev.* **1992**, 179−185. (b) Drago, R. S. *Coord. Chem. Rev.* **1992**, *117*, 185−213.

(5) Leung, K. S. Y.; Wong, W. T. *J. Chem. Soc., Dalton Trans.* **1997**, 4357−4360.

(6) Wong, J. S. Y.; Wong, W. T. *New J. Chem.* **2002**, *26*, 94−104.

(7) (a) Amoroso, A. J.; Gade, L. H.; Johnson, B. F. G.; Lewis, J.; Raithby, P. R.; Wong, W. T. *Angew. Chem., Int. Ed. Engl.* **1991**, *30*, 107−109. (b) Johnson, B. F. G.; Gade, L. H.; Lewis, J.; Wong, W. T. *Mater. Chem. Phys.* **1991**, *29*, 85−96. (c) Gade, L. H.; Johnson, B. F. G.; Lewis, J.; McPartlin, M.; Powell, H. R.; Raithby, P. R.; Wong, W. T. *J. Chem. Soc., Dalton Trans.* **1994**, 521−532. (d) Amoroso, A. J.; Johnson, B. F. G.; Lewis, J.; Raithby, P. R.; Wong, W. T. *J. Chem. Soc., Chem. Commun.* **1991**, 814−815. (e) Amoroso, A. J.; Johnson, B. F. G.; Lewis, J.; Raithby, P. R.; Wong, W. T. *Angew. Chem., Int. Ed. Engl.* **1991**, *30*, 1505−1506. (f) Amoroso, A. J.; Johnson, B. F. G.; Lewis, J.; Raithby, P. R.; Wong, W. T. *J. Indian Chem. Soc.* **1993**, *70*, 967−973.

10.1021/om030271t CCC: $25.00
Publication on Web 10/10/2003

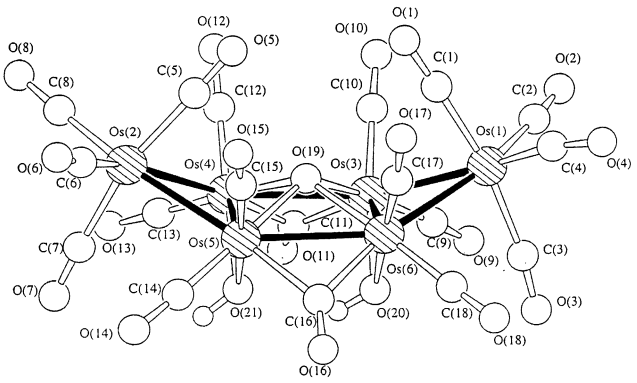

Figure 1. Molecular structure of **1** showing the atom-numbering scheme.

Table 1. Selected Bond Lengths (Å) and Angles (deg) for 1

Os(1)−Os(3)	2.796(1)	Os(3)−O(19)	2.20(1)
Os(1)−Os(6)	2.807(1)	Os(3)−O(20)	2.10(1)
Os(2)−Os(4)	2.805(1)	Os(4)−O(19)	2.19(1)
Os(2)−Os(5)	2.805(1)	Os(4)−O(21)	2.09(1)
Os(3)−Os(4)	2.789(1)	Os(5)−O(19)	2.20(1)
Os(3)−Os(6)	2.981(1)	Os(5)−O(21)	2.16(1)
Os(4)−Os(5)	2.986(1)	Os(6)−O(19)	2.17(2)
Os(5)−Os(6)	2.809(1)	Os(6)−O(20)	2.13(1)
Os(1)−Os(3)−Os(6)	58.04(3)	Os(3)−Os(4)−Os(5)	89.89(3)
Os(1)−Os(6)−Os(3)	57.66(3)	Os(3)−Os(6)−Os(5)	89.61(3)
Os(2)−Os(5)−Os(4)	57.85(3)	Os(4)−Os(2)−Os(5)	64.32(3)
Os(2)−Os(4)−Os(5)	57.83(3)	Os(4)−Os(3)−Os(6)	90.43(3)
Os(3)−Os(1)−Os(6)	64.30(3)	Os(4)−Os(5)−Os(6)	89.95(3)

bridged by carbonyl ligands, while those of the opposite edges with bridging hydroxy groups Os(3)−Os(4) and Os(5)−Os(6) are similar [2.789(1) vs 2.809(1) Å]. The four osmium atoms are capped by a quadruply bridging oxo ligand with an average Os−O distance of 2.19(3) Å and an out-of-plane distance of 0.787 Å. The μ_4-oxo moiety exhibits a coordination mode that is similar to those found in the undecaosmium cluster $[Os_{11}(\mu_4\text{-O})_3(CO)_{30}]$,[1b] where the oxygen atoms lie above the square osmium plane by 0.70 Å, with an average Os−O distance of 2.17 Å. In **1**, two additional $Os(CO)_4$ fragments are found to bridge the opposite edges Os(3)−Os(6) and Os(4)−Os(5) such that they both flap above the basal plane toward the side of the oxo ligand to form a distorted boat form metal core. The two planes, Os(1)−Os(3)−Os(6) and Os(2)−Os(4)−Os(5), form dihedral angles of 24.98° and 27.42° with the basal tetraosmium plane, respectively. The capping modes of μ_3-oxo[1e,5] or μ_4-oxo[1b,6] in osmium cluster systems have been reported.

The presence of hydrogen atoms on the hydroxyl ligands in **1** was confirmed by the observation of two O−H stretching vibrations that occurred at 3689w and 3675w cm^{-1} in its IR spectrum. The ^1H NMR spectrum of **1** showed only a broad single resonance (δ −0.40) for the hydroxyl hydrogen atoms, which suggests that they were rapidly interchanging their environments. An example in the ruthenium system with a structure that is similar to **1**, $[Ru_6(CO)_{16}(\mu\text{-CO})_2(\mu\text{-OH})_2(\mu_4\text{-S})]$, has also been observed.[8] The molecular structure of **1** differs from that of the ruthenium cluster by the replacement of the ruthenium atoms and the μ_4-S ligand with osmium atoms and a μ_4-oxo ligand, respectively. However, to the best of our knowledge there is no structurally characterized example of a μ_4-oxo hexanuclear cluster with a boat form metal framework in the osmium system.

(8) Adams, R. D.; Babin, J. E.; Tasi, M. *Inorg. Chem*. **1987**, *26*, 2561−2563.

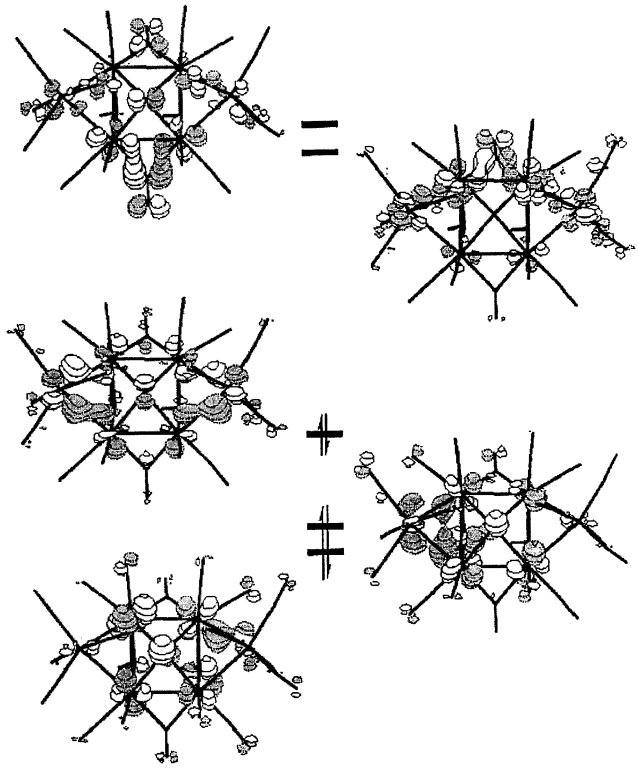

Figure 2. Contour plots of the lowest unoccupied (LUMO) and the highest occupied (HOMO) molecular orbitals calculated for **1**.

Assuming that the μ_4-oxo group behaves as a four-electron donor, electron counting indicates that **1** has 94 valence electrons rather than 92, which is expected for a boat form metal cluster with eight metal−metal bonds. According to Adams et al.,[8] the two surplus electrons are supposed to occupy a delocalized antibonding orbital of the tetranuclear metal plane, which results in a weakening of the four associated metal−metal bonds within the square base. A density functional calculation at the B3LYB level has been performed on **1** on the basis of the experimetally determined geometry. It suggests that the two Os−Os bonds with bridging hydroxy units in **1** are much weaker than the others because the two σ^* antibonding orbitals that correspond to the two hydroxy-bridged Os−Os bonds are occupied by the excess electrons. The average bond index for the two hydroxy-bridged Os−Os bonds is 0.06, while the bond indices for all other bonds range from 0.10 to 0.23. Consistent with this is the observed average bond distance of the two weakened Os−Os bonds at 2.984(1) Å, while that of the others is 2.802(2) Å. The same structural feature can be observed in $[Ru_6(CO)_{16}(\mu\text{-CO})_2(\mu\text{-OH})_2(\mu_4\text{-S})]$.[8]

To understand the spectroscopic features of **1**, the molecular orbitals that are located in the frontier region have been plotted. The contour plots of three highest occupied and two lowest unoccupied molecular orbitals are shown in Figure 2. Though there are extensive mixings in these orbitals, their properties can be described qualitatively. The highest occupied molecular

orbital (HOMO) mainly corresponds to the edge-bridged Os−Os bonding. The second and third HOMOs are related to the "t_{2g}" sets from the Os centers and show significant contributions from those atomic orbitals, which are supposed to accommodate the lone pair electrons of the μ_4-O and μ-OH ligands. The two lowest unoccupied molecular orbitals (LUMOs) are mainly from the π^* orbitals of the bridging carbonyls and show some Os−Os σ^* character. On the basis of the properties of these frontier orbitals, the two absorption peaks observed in the UV−vis spectrum can be assigned as follows. The weaker peak in the visible region (561 nm) is due to the HOMO to LUMO transition, which possesses the mixed feature of d−d and metal(d)-to-ligand-(π^* of the bridging carbonyls) charge transfer. The stronger peak in the UV region is due to the transition of the second and third HOMOs to the LUMOs, which has the mixed feature of metal(d)-to-ligand(π^* of the bridging carbonyls) and ligand(lone pairs of the bridging oxo)-to-ligand(π^* of the bridging carbonyls) charge transfers.

Vacuum Pyrolysis of $[Os_6(CO)_{16}(\mu_4\text{-}O)(\mu\text{-}OH)_2(\mu\text{-}CO)_2]$, 1. Heating the hexaosmium cluster **1** at 200 °C in a sealed tube for 2 h yielded the new binary dodecaosmium cluster $[Os_{12}(CO)_{30}]$, **2**, in 32% yield. Other known products in this reaction were $[Os_4O_4(CO)_{12}]$ (15%), $[Os_5(CO)_{16}]$ (5%), $[Os_6(CO)_{18}]$ (10%), $[Os_7(CO)_{21}]$ (5%), and $[Os_8(CO)_{23}]$ (8%). Similar observations were obtained when the reaction was conducted in the temperature range 200−280 °C. No reaction occurred and approximately 90% of the starting cluster was recovered when the temperature of the pyrolysis was below 200 °C. The molecular structure of **2** was established by an X-ray analysis and is depicted in Figure 3a. Selected bond lengths of **2** are given in Table 2.

Cluster **2** contains a novel metal core of 12 osmium atoms (Figure 3b). The Os_{12} metallic array exhibits a quite irregular geometry, without any high-symmetry elements. The structure of **2** can be described as a distorted central square pyramid [Os(1)−Os(6)−Os(7)−Os(8)−Os(9)] with three tetrahedra [Os(2)−Os(6)−Os(7)−Os(10), Os(4)−Os(8)−Os(9)−Os(11), and Os(5)−Os(6)−Os(9)−Os(12)] joined to it by sharing three edges [Os(6)−Os(7), Os(8)−Os(9), and Os(6)−Os(9)], respectively, and together with one osmium atom Os(3) capping a triangular face of the pyramid [Os(1)−Os(7)−Os(8)] (average Os−Os distance of 2.76 Å.) The three vertexes of the tetrahedra are coordinated to the apical atom Os(1) of the central pyramid. There is a long Os−Os bond between the two tetrahedral vertexes [Os(4)−Os(5) 3.089 Å]. Cluster **2** has an overall electron count of 156, which is consistent with that predicted from the EAN rule for a metal cluster with 30 metal−metal bonds. The metal arrangement in **2** has never been observed in high-nuclearity clusters. Dodecanuclear clusters of transition metals (Pd, Ir, Rh) have been reported. Their metal cores exhibit different geometry, including a hexacapped distorted octahedron,[9] a distorted icosahedron,[10] a ν_2 trigonal bipyramid that lacks two of the vertexes,[11] and two prismatic units that share an edge plus two extra metal atoms capping the facing square faces of the prisms.[12] Cluster **2** is the largest neutral binary osmium carbonyl complex that has been structurally characterized.

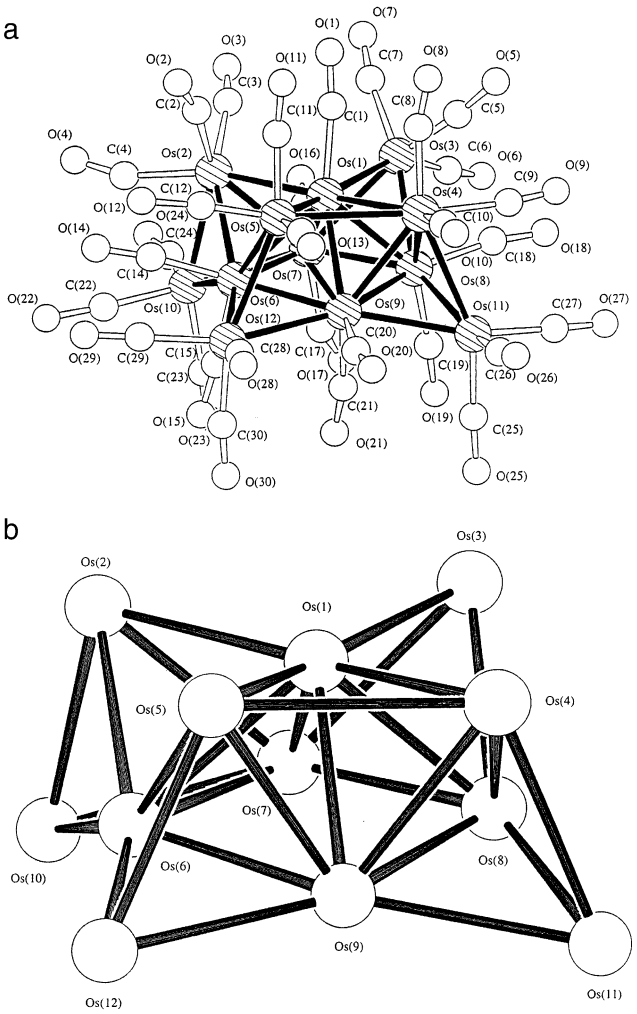

Figure 3. (a) Molecular structure of **2** showing the atom-numbering scheme. (b) Metal core geometry of **2**.

Table 2. Selected Bond Lengths (Å) for 2

Os(1)−Os(2)	2.816(2)	Os(5)−Os(6)	2.943(2)
Os(1)−Os(3)	2.752(2)	Os(5)−Os(9)	2.725(2)
Os(1)−Os(4)	2.772(2)	Os(5)−Os(12)	2.859(3)
Os(1)−Os(5)	2.727(2)	Os(6)−Os(7)	2.885(2)
Os(1)−Os(6)	2.628(2)	Os(6)−Os(9)	2.761(2)
Os(1)−Os(7)	2.594(2)	Os(6)−Os(10)	2.914(2)
Os(1)−Os(8)	2.572(2)	Os(6)−Os(12)	2.773(3)
Os(1)−Os(9)	2.865(2)	Os(7)−Os(8)	2.763(2)
Os(2)−Os(6)	2.770(2)	Os(7)−Os(10)	2.692(2)
Os(2)−Os(7)	2.770(2)	Os(8)−Os(9)	2.764(2)
Os(2)−Os(10)	2.818(2)	Os(8)−Os(11)	2.740(2)
Os(3)−Os(7)	2.749(2)	Os(9)−Os(11)	2.792(2)
Os(3)−Os(8)	2.789(2)	Os(9)−Os(12)	2.780(2)
Os(4)−Os(5)	3.089(2)	Os(2)···Os(3)	3.993(2)
Os(4)−Os(8)	2.894(2)	Os(2)···Os(5)	4.242(2)
Os(4)−Os(9)	2.706(2)	Os(3)···Os(4)	4.205(2)
Os(4)−Os(11)	2.902(2)		

Electrochemistry. To investigate the redox properties of the hexaosmium oxo cluster, the electrochemistry

(9) Mednikov, E. G.; Struchkov, Y. T.; Slovokhotov, Y. L. *J. Organomet. Chem*. **1998**, *566*, 15−20.
(10) Vidal, J. L.; Troup, J. M. *J. Organomet. Chem*. **1981**, *213*, 351−363.
(11) Pergola, R. D.; Demartin, F.; Garlaschelli, L.; Manassero, M.; Martinengo, S.; Masciocchi, N.; Zanello, P. *Inorg. Chem*. **1993**, *32*, 3670−3674.
(12) (a) Albano, V. G.; Braga, D.; Chini, P.; Strumolo, D.; Martinengo, S. *J. Chem. Soc., Dalton Trans*. **1983**, 249−252. (b) Albano, V. G.; Braga, D.; Strumolo, D.; Seregni, C.; Martinengo, S. *J. Chem. Soc., Dalton Trans*. **1985**, 1309−1313.

of cluster **1** was examined. Cyclic voltammetry and controlled potential coulometry were carried out at 298 K in a standard three-electrode system[13] (glassy carbon/carbon cloth working electrode, platinum auxiliary electrode and $Ag/AgNO_3$ reference electrode) using 0.1 M tetrabutylammonium hexafluorophosphate−dichloromethane solution as the supporting electrolyte.

Cluster **1** exhibited an irreversible cathodic wave (E_{pc}) at −1.00 V vs $Ag/AgNO_3$, along with weak oxidation at −0.92 V. The region where the weak oxidation wave appeared was initially empty, and the wave appearing after the cathodic wave was traversed. An additional irreversible anodic wave was observed at $E_{pa} = 0.69$ V. Controlled potential coulometry in correspondence with the cathodic process ($E_w = -1.04$ V) showed that it involves the consumption of 1 Faraday/mol of **1**. Increased scan rates did not lead to any noticeable reversibility of this 0/−1 redox couple. It presumably derived from an irreversible fast chemical reaction that followed the reduction (i.e., an EC process). On the basis of the relative peak currents of the cathodic and anodic waves, the oxidation process is also assigned as a one-electron step. Because the molecular orbital calculations of **1** show that the LUMOs contain mainly π^* of the bridging carbonyls, it is reasonable to observe a reduction peak in the cyclic voltammogram as the chance of fragmentation is significantly reduced.

Experimental Section

General Procedures. The solvents were of reagent grade and dried by distillation over the appropriate drying agents under nitrogen prior to use.[14] The separation and purification of products were achieved by preparative thin-layer chromatography (TLC) glass plates (20 cm × 20 cm) that were precoated with Merck Kieselgel 60 GF_{254} prepared in this laboratory (0.7 mm) or from a commercial source (0.25 mm). TLC was carried out in air using solvents of laboratory grade as eluents. Infrared spectra were recorded on a Bio-Rad FTS-135 IR spectrometer, using 0.5 mm calcium fluoride solution cells. ^{1}H NMR spectra were recorded on a Bruker DPX 300 NMR spectrometer using CD_2Cl_2 with reference to $SiMe_4$ (δ 0). Mass spectra were obtained on a Finnigan MAT 95 mass spectrometer by fast atom bombardment techniques, using *m*-nitrobenzyl alcohol as the matrix solvent. Electronic absorption spectra were obtained with a Hewlett-Packard 8453 diode array UV/vis spectrophotometer, using quartz cells, with a 1 cm path length at room temperature. Microanalyses were performed by Butterworth Laboratories, UK.

Materials. All chemicals, unless otherwise stated, were purchased commercially and used as received. $[Os_3(CO)_{11}(NCMe)]$ was prepared by the literature method.[15]

$[Os_6(CO)_{16}(\mu_4\text{-}O)(\mu\text{-}OH)_2(\mu\text{-}CO)_2]$, 1. $[Os_3(CO)_{11}(NCMe)]$ (63 mg, 0.068 mmol) was dissolved in 30 mL of octane. When a continuous oxygen stream was bubbled through the solution, for 15 min, under reflux, a brown solution was obtained. Evaporation to dryness and separation of the residue by TLC using *n*-hexane−CH_2Cl_2 (1:1 v/v) gave the purple cluster **1** ($R_f \approx 0.15$, 32 mg, 55%). Spectroscopic data for **1**: IR [ν(CO), CH_2Cl_2]: 2120w, 2089s, 2049s, 2033m, 1983w, 1846w-(KBr), 1816w(KBr) cm^{-1}. IR [ν(OH), KBr]: 3689w, 3675w cm^{-1}. λ_{max} (nm) (ϵ, 10^{-3} dm^3 mol^{-1} cm^{-1}) in CH_2Cl_2 at 298 K: 229 (28.8), 349 (24.2), 561 (13.1). ^{1}H NMR (CD_2Cl_2): δ −0.40 (s, 2H). Positive FAB mass spectrum: *m*/*z* 1695 (1695 calcd). Anal. Calcd (%) for $C_{18}H_2O_{21}Os_6$: C, 12.75; H, 0.12. Found: C, 12.75; H, 0.15.

Table 3. Summary of Crystal Data and Data Collection Parameters for 1 and 2

	1	**2**
empirical formula	$C_{18}H_2O_{21}Os_6 \cdot CH_2Cl_2$	$C_{30}O_{30}Os_{12}$
fw	1780.33	3122.71
cryst color, habit	purple, block	dark green, block
cryst dimens/mm	0.19 × 0.22 × 0.23	0.21 × 0.23 × 0.25
cryst syst	monoclinic	orthorhombic
space group	$P2_1$ (#4)	$P2_12_12_1$ (#19)
a/Å	11.819(2)	11.740(2)
b/Å	10.423(2)	18.361(3)
c/Å	13.125(2)	24.542(4)
α/deg		
β/deg	94.59(3)	
γ/deg		
U/Å^3	1611.7(4)	5290(1)
Z	2	4
D_{calc}/g cm^{-3}	3.668	3.920
F(000)	1552.00	5328.00
μ(Mo Kα)/cm^{-1}	237.94	287.54
no. of reflns collected	9912	33365
no. of unique reflns	3773	6684
obsd reflns [$I > 1.5\sigma(I)$]	3480	4912
weighting scheme	$w = [\sigma^2(F_o)]^{-1}$	$w = [\sigma^2(F_o)]^{-1}$
p-factor	0.0440	0.0440
R	0.040	0.055
R_w	0.043	0.058
goodness of fit, *S*	1.15	1.17
max. Δ/σ	0.00	0.00
no. of params	248	349
residual extrema in the final ΔF map/e Å^{-3}	2.41, −2.06	2.73, −2.16

$[Os_{12}(CO)_{30}]$, 2. A CH_2Cl_2 solution (5 mL) of **1** (100 mg, 0.059 mmol) was introduced into a Carious tube. The solvent was removed under reduced pressure, and the tube was sealed after being dried. The compound was pyrolyzed at 220 °C for 2 h to give a dark brown powder together with a small amount of colorless crystals. The colorless crystals were isolated and found to be $[Os_4O_4(CO)_{12}]$ (15 mg, 15%) according to the spectroscopic and crystallographic data. The residue was extracted exhaustively with CH_2Cl_2, and after concentration the combined extracts were subjected to preparative TLC separation. Elution with *n*-hexane−CH_2Cl_2 (3:1 v/v) afforded cluster **2** ($R_f \approx 0.40$, 29 mg, 32%), $[Os_5(CO)_{16}]$ ($R_f \approx 0.80$, 5 mg, 5%), $[Os_6(CO)_{18}]$ ($R_f \approx 0.75$, 10 mg, 10%), $[Os_7(CO)_{21}]$ ($R_f \approx 0.65$, 5 mg, 5%), and $[Os_8(CO)_{23}]$ ($R_f \approx 0.60$, 8 mg, 8%). Spectroscopic data for **2**: IR [ν(CO), CH_2Cl_2]: 2095vs, 2084m, 2064w, 2037m, 2022m cm^{-1}. ^{1}H NMR (CD_2Cl_2): no hydride signal detected. Positive FAB mass spectrum: *m*/*z* 3123 (3123 calcd). Anal. Calcd (%) for $C_{30}O_{30}Os_{12}$: C, 11.54. Found: C, 11.54.

Electrochemical Studies. Electrochemical measurements were performed with an EG & G Princeton Applied Research (PAR) model 273A potentiostat, which was connected to an interfaced computer employing PAR 270 electrochemical software. Cyclic voltammograms were obtained with a gas (argon) sealed two-compartment cell equipped with a glassy carbon working electrode (Bioanalytical), a platinum wire auxiliary electrode (Aldrich), and $Ag/AgNO_3$ reference (Bioanalytical) electrodes at room temperature. *n*-Tetrabutylammonium hexafluorophosphate (0.1 mol dm^{-3}, TBAHFP) in anhydrous deoxygenated CH_2Cl_2 was used as a supporting electrolyte. Ferrocene was added at the end of each experiment as an internal standard. Potential data (vs $Ag/AgNO_3$) were checked against the ferrocene (0/+1) couple; under the actual experimental conditions the ferrocene/ferrocenium couple was located at +0.13 V. Bulk electrolyses were carried out in a gastight

(13) Heinze, J. *Angew. Chem., Int. Ed. Engl.* **1984**, *11*, 831.
(14) Perrin, D. D.; Armarego, W. L. F. *Purification of Laboratory Chemicals*, 3rd ed.; Pergamon: Oxford, 1988.
(15) Nicholls, J. N.; Vargas, M. D. *Inorg. Synth.* **1989**, *28*, 232.

cell consisting of three chambers that were separated at the bottom by fine frits, with a carbon cloth (80 mm^2) working electrode in the middle and $Ag/AgNO_3$ reference and Pt gauze auxiliary electrodes in the lateral chambers. The working potentials (E_w) for reduction and oxidation processes were ca. 0.15 V more negative and more positive than the corresponding electrode potential (E_p), respectively; all of the coulometric experiments were completed in duplicate.

Crystallography. Crystals suitable for X-ray analyses were glued on glass fibers with epoxy resin. The intensity data of the crystals were collected at ambient temperature using a Bruker SMART CCD 1000 diffractometer equipped with graphite-monochromated Mo Kα radiation. The diffracted intensities were corrected for Lorentz and polarization effects. Absorption corrections were applied by SADABS. The structures were solved by direct methods (SIR 92[16] for **1** and SHELXS 86[17] for **2**) and expanded by Fourier difference techniques (DIRDIF94).[18] The atomic coordinates and thermal parameters were refined by full-matrix least-squares analysis on *F*, with anisotropic displacement parameters for non-hydrogen atoms whenever possible. Hydrogen atoms were generated in their ideal positions and included in the structure factor calculations, but not refined. All calculations were performed using the TeXsan[19] software package on a Silicon-Graphics computer. Summaries of crystal data, data collection parameters, and structure solution and the final structural details for all determined structures are collectively listed in Table 3.

Crystallographic data (excluding structure factors) for the structures that are reported in this paper have been deposited with the Cambridge Crystallographic Data Centre as supplementary publication nos. CCDC 201079 and CCDC 201080. Copies of the data can be obtained free of charge on application to CCDC, 12 Union Road, Cambridge, CB2 1EZ (fax: (+44) 1223-336-408; e-mail: deposit@ccdc.cam.ac.uk).

Acknowledgment. We gratefully acknowledge financial support from the Hong Kong Research Grants Council and The University of Hong Kong. J.S.-Y.W. acknowledges the receipt of a Postgraduate Studentship, Hung Hing Ying Scholarship, and Hui Pui Hing Scholarship administered by The University of Hong Kong, and Sir Edward Youde Memorial Fellowship awarded by the Sir Edward Youde Memorial Trustees.

Supporting Information Available: Text giving crystallographic data for **1** and **2**. This material is available free of charge via the Internet at http://pubs.acs.org.

OM030271T

(16) Altomare, A.; Burla, M. C.; Camalli, M.; Cascarano, M.; Giacovazzo, G.; Guagliardi, A.; Polidori, G. SIR 92. *J. Appl. Crystallogr.* **1994**, *27*, 435.

(17) Sheldrick, G. M. In *Crystallographic Computing 3*; Sheldrick, G. M., Kruger, C., Goddard, R., Eds.; Oxford University Press: Oxford, 1985; p 175.

(18) Beurskens, B. T.; Admiroal, G.; Beurskens, G.; Bosman, W. P.; de Gelder, R.; Isrel, R.; Smits, J. M. M. *DIRDIF94*; Technical Report of the Crystallographic Laboratory; University of Nijmegen, 1994.

(19) *teXsan*: Crystal Structure Analysis Package; Molecular Structure Corporation: The Woodlands, TX, 1985 and 1992.